Competitive Adsorption and Diffusion of Gases in a Microporous Solid

Mykhaylo Petryk, Mykola Ivanchov, Sebastian Leclerc, Daniel Canet, Jacques Fraissard

Chapter

Competitive Adsorption and Diffusion of Gases in a Microporous Solid

Mykhaylo Petryk, Mykola Ivanchov, Sebastian Leclerc, Daniel Canet and Jacques Fraissard

Abstract

The experimental and theoretical study of the co-adsorption and co-diffusion of several gases through a microporous solid and the instantaneous (out of equilibrium) distribution of the adsorbed phases is particularly important in many fields, such as gas separation, heterogeneous catalysis, purification of confined atmospheres, reduction of exhaust emissions contributing to global warming, etc. The original NMR imaging technique used gives a signal characteristic of each adsorbed gas at each instant and at each level of the solid and therefore the distribution of several gases in competitive diffusion and adsorption. But it does not allow to determine separately the inter- and intra-crystallite quantities. A new fast and accurate analytical method for the calculation of the coefficients of co-diffusing gases in the intra- and inter-crystallite spaces of microporous solid (here ZSM 5 zeolite) is developed, using high-performance methods (iterative gradient methods of residual functional minimization and analytical methods of influence functions) and mathematical co-adsorption models, as well as the NMR spectra of each adsorbed gas in the bed. These diffusion coefficients and the gas concentrations in the inter- and intra-crystallite spaces are obtained for each position in the bed and for different adsorption times.

Keywords: competitive diffusion of gases, competitive adsorption, modeling, diffusion coefficient, Heaviside's operational method, zeolite bed, gradient methods of identification

1. Introduction

Knowledge of the co-diffusion and co-adsorption coefficients of reactants and products is essential when a heterogeneous catalytic reaction is performed by flowing gases through a microporous catalyst bed. But generally the distribution of the various reactants adsorbed on the catalyst is very inhomogeneous and, moreover, very variable from one reactant to another. It is therefore necessary to determine at every moment the diffusion coefficient of each reactant in the presence of the others and its instantaneous distribution along the length of the catalyst bed.

Classical H-MRI should be a good technique for monitoring the co-diffusion and co-adsorption of several gases flowing through a microporous bed. However, since the signal obtained is not specific for each gas, this requires that each experiment be performed several times under identical conditions and each time with only one not deuterated gas. To remedy the drawbacks of classical imaging, we have used the NMR

imaging technique, named slice selection procedure, to follow the diffusion and adsorption of a gas in a microporous bed [1–3]. The sample is displaced vertically, step-by-step, relative to a very thin coil detector during the adsorption of the gas. The bed is assumed to consist of *N* very thin layers of solid, and the region probed is limited to each layer, so that the variation of the concentration of gas absorbed at the level of each layer is obtained as a function of time. An interesting feature of this technique is its ability to visualize directly the co-diffusion of several gases. Indeed, the NMR signals are quantitatively characteristic of the adsorbed gases. They can therefore provide directly, at every moment and at every level of the bed, the distribution of several gases competing in diffusion and adsorption. We have presented in a previous paper the experimental results of the co-diffusion of benzene and hexane through a silicalite bed [4]. In [5, 6] we have developed a mathematical methodology for efficient linearization of similar models. Using Heaviside's operational method and Laplace's integral transformation method, we have built solutions allowing fast calculations for two-component co-adsorption in a heterogeneous zeolite bed and for the dehydration of natural gas [7]. In this chapter we have improved the methods previously used to compute the diffusion coefficients against time, increasing the accuracy and speed of calculations by significantly reducing the iteration number. This made it possible to use them for the co-adsorption of several gases diffusing along such a column.

2. Experimental

The NMR imaging technique, the sample-holder bulb containing the liquid phase in equilibrium with the gas phase, and the narrow zone monitored by the detector have been described in [1–3], respectively.

The upper face of the cylindrical bed of zeolite crystallites is exposed to a constant pressure of each gas (**Figure 1**). The diffusion of the two gases is axial in

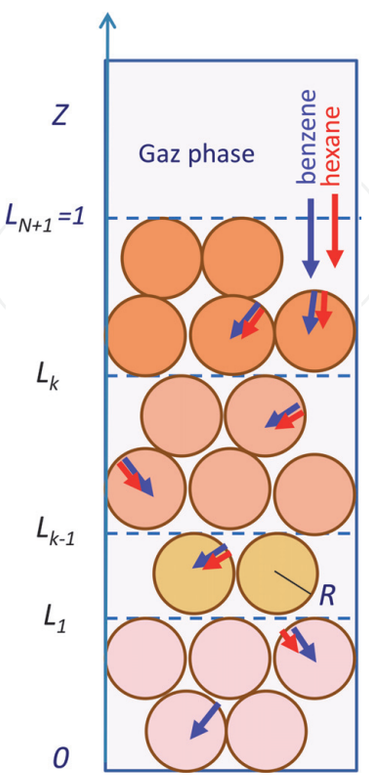

Figure 1.
Distribution of the layers (left) and corresponding parameters (right).

the macropores of the inter-crystallite space (z direction along the height, l, of the bed) and radial in the micropores of the zeolite. According to the experimental conditions, the zeolite bed consists of a large number, N, of very thin layers of solid, of thickness $\Delta l_k = l_k - l_{k-1}$, perpendicular to the propagation of the gas in the z direction. The corresponding coefficients of inter- and intra-crystallite space are $D_{inter,k}$ and $D_{intra,k}$, respectively.

3. Experimental results: gaseous benzene and hexane adsorption curves

The experimental results have been summarized in [4]: the spectrum of each gas at every instant and every level of the solid and the benzene and hexane concentrations along the sample, for each diffusion time. Here we shall only use the evolution, as a function of time, of the benzene and hexane concentrations at different levels of the sample, on which the calculations of the diffusion coefficients and the instantaneous inter- and intra-crystallite concentrations are based [8]. **Figure 2** shows clearly that, under the chosen experimental conditions, benzene hinders the diffusion of hexane, and this at every moment. Moreover, it can be noticed that, at equilibrium, the amount of benzene within the zeolite is twice that of hexane, indicating quantitatively the relative affinity to the two adsorbates.

These curves display modulations as a function of time, which must be averaged for all subsequent mathematical representations. These modulations are weak at the lower layers of the tube and can be due to errors in the measurement of small amounts. Those closer to the arrival of the gas are greater and are similar for the two gases. We suggested that these fluctuations may be due to the fact that inter-crystallite adsorption at levels close to the gas phase is fast compared to the liquid-gas equilibrium, which is not as instantaneous for a mixture as for a single component [8]. Each slight decrease of the gas pressure could correspond a slight fast desorption.

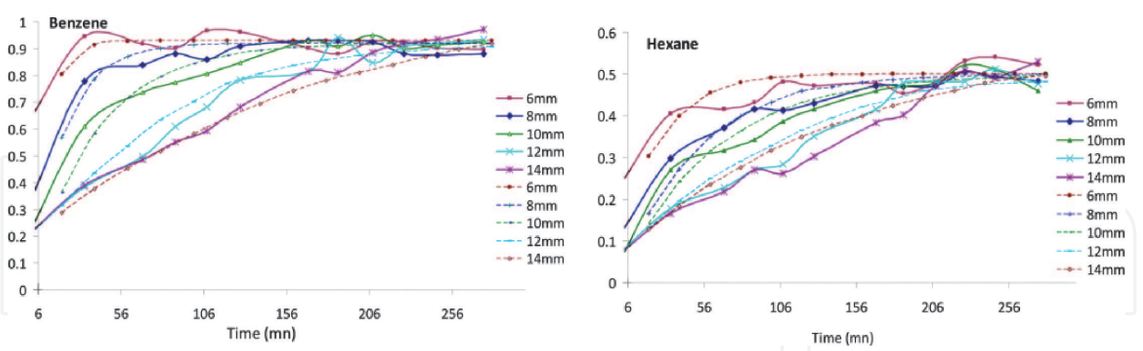

Figure 2.
*Evolution vs. time of the benzene and hexane concentrations (arbitrary units) at different levels of the sample (*continuous*, experimental curves;* dotted*, their approximations used for simulation) [from Ref. [8], reprinted with permission from ACS].*

4. A mathematical model of competitive co-adsorption and co-diffusion in microporous solids

4.1 Co-adsorption model in general formulation

The model presented is similar to the bipolar model [2, 3, 8, 9]. By developing the approach described by Ruthven and Kärger [10, 11] and Petryk et al. [5]

concerning the elaboration of a complex process of co-adsorption and co-diffusion, it is necessary to specify the most important hypotheses limiting the process.

The general hypothesis adopted to develop the model presented in the most general formulation is that the interaction between the co-adsorbed molecules of several gases and the adsorption centers on the surface in the nanoporous crystallites is determined by the nonlinear competitive equilibrium function of the Langmuir type, taking into account physical assumptions [10]:

1. Co-adsorption is caused by the dispersion forces whose interaction is established by Lennard-Jones and the electrostatic forces of gravity and repulsion described by van der Waals [11].

2. The co-diffusion process involves two types of mass transfer: diffusion in the macropores (inter-crystallite space) and diffusion in the micropores of crystallites (intra-crystallite space).

3. During the evolution of the system toward equilibrium, there is a concentration gradient in the macropores and/or in the micropores.

4. Co-adsorption occurs on active centers distributed over the entire inner surface of the nanopores (intra-crystallite space) [10, 11]. All crystallites are spherical and have the same radius R; the crystallite bed is uniformly packed.

5. Active adsorption centers adsorb molecules of the *i*th adsorbate, forming molecular layers of adsorbate on their surfaces.

6. Adsorbed molecules are held by active centers for a certain time, depending on the temperature of the process.

Taking into account these hypotheses, we have developed a nonlinear co-adsorption model. The meaning of the symbols is given in the nomenclature:

$$\frac{\partial C_s(t,Z)}{\partial t} = \frac{D_{\text{inter}_s}}{l^2}\frac{\partial^2 C_s}{\partial Z^2} - e_{\text{inter}}\tilde{K}_s\frac{D_{\text{intra}_s}}{R^2}\left(\frac{\partial Q_s}{\partial X}\right)_{X=1} \tag{1}$$

$$-H\frac{\partial T(t,z)}{\partial t} - uh_g\frac{\partial T}{\partial z} - \sum_{s=1}^{m}\Delta\overline{H}_s\frac{\partial\overline{Q}_s}{\partial t} - 2\frac{\alpha_h}{R_{column}}T + \Lambda\frac{\partial^2 T}{\partial z^2} = 0 \tag{2}$$

$$\frac{\partial Q_s(t,X,Z)}{\partial t} = \frac{D_{\text{intra}_s}}{R^2}\left(\frac{\partial^2 Q_s}{\partial X^2} + \frac{2}{X}\frac{\partial Q_s}{\partial X}\right) \tag{3}$$

with initial conditions

$$C_s(t=0,Z) = 0; Q_s(t=0,X,Z) = 0; Z\in(0,1), X\in(0,1), s = \overline{1,\text{m}} \tag{4}$$

boundary conditions for coordinate X of the crystallite

$$\frac{\partial}{\partial X}Q_s(t,X=0,Z) = 0\ \left(\text{symmetry conditions}\right), \tag{5}$$

$$Q_s(t,X=1,Z) = \frac{K_s(T)C_s(t,Z)}{1+\sum\limits_{s_1=1}^{m}K_{s_1}(T)C_{s_1}(t,Z)}, s = \overline{1,\text{m}}\ (\text{Langmuir equilibrium}), \tag{6}$$

boundary and interface conditions for coordinate Z

$$C_s(t,1)=1,\ \frac{\partial C_s}{\partial Z}(t,Z=0)=0,t>0 \tag{7}$$

$$T(t,\mathrm{Z})\Big|_{Z=1}=T_{initial},\frac{\partial}{\partial z}T(t,\mathrm{Z})|_{Z=0}=0. \tag{8}$$

with $K_s(T)=k_{0s}\exp\left(-\frac{\Delta H_s}{R_gT}\right)$.

Here the activation energy is the heat of adsorption defined as$\Delta H_s=\overline{\phi}-\left(U_{g_s}-U_{ads_s}\right)-R_gT$, where $U_{g_s}-U_{ads_s}$—the difference between the kinetic energies of the molecule of the *i*th component of the adsorbate in the gaseous and adsorbed states is the magnitude of the Lennard-Jones potential, averaged over the pore volume of the adsorbent [11].

The non-isothermal model (1)–(8) can easily be transformed into isothermal model, removing the temperature Eq. (2) and condition (8) and replacing the functions $K_s(T)$ with the corresponding equilibrium constants K_s. The competitive diffusion coefficients D_{intra_s} and D_{inter_s} can be considered as functions of the time and the position of the particle in the zeolite bed.

4.2 The inverse model of co-diffusion coefficient identification: application to the benzene-hexane mixture

On the basis of a developed nonlinear co-adsorption model (1)–(8) , we construct an inverse model for the identification of the competitive diffusion coefficients D_{intra_s} and D_{inter_s} as a function of time and coordinate in the zeolite bed.

The mathematical model of gas diffusion kinetics in the zeolite bed is defined in domains: $\Omega_{k_t}=\left(0,t^{total}\right)\times\Omega_k$, $\left(\Omega_k=(L_{k-1},L_k),k=\overline{1,N+1},L_0=0<L_1<\ldots<L_{N+1}=1\right)$ by the solutions of the system of differential equations

$$\frac{\partial C_{s_k}(t,Z)}{\partial t}=\frac{D_{\mathrm{inter}_{s_k}}}{l^2}\frac{\partial^2 C_{s_k}}{\partial Z^2}-e_{\mathrm{inter}_k}\tilde{K}_{s_k}\frac{D_{\mathrm{intra}_{s_k}}}{R^2}\left(\frac{\partial Q_{s_k}}{\partial X}\right)_{X=1} \tag{9}$$

$$\frac{\partial Q_{s_k}(t,X,Z)}{\partial t}=\frac{D_{\mathrm{intra}_{s_k}}}{R^2}\left(\frac{\partial^2 Q_{s_k}}{\partial X^2}+\frac{2}{X}\frac{\partial Q_{s_k}}{\partial X}\right) \tag{10}$$

with initial conditions

$$C_{s_k}(t=0,Z)=0;Q_{s_k}(t=0,X,Z)=0;X\in(0,1),Z\in\Omega_k,k=\overline{1,N+1}, \tag{11}$$

boundary and interface conditions for coordinate Z

$$C_{s_1}(t,L_1)=1,\ \frac{\partial C_{s_1}}{\partial Z}(t,Z=0)=0,t\in\left(0,t^{total}\right); \tag{12}$$

$$\left[C_{s_k}(t,Z)-C_{s_k}(t,Z)\right]_{Z=L_k}=0,\ \frac{\partial}{\partial Z}\left[D_{\mathrm{inter}_{s_{k-1}}}C_{s_{k-1}}(t,Z)-D_{\mathrm{inter}_{s_k}}C_{s_k}(t,Z)\right]_{Z=L_k}=0,k=\overline{1,N},t\in\left(0,t^{total}\right); \tag{13}$$

boundary conditions for coordinate X in the particle

$$\frac{\partial}{\partial X} Q_{s_k}(t, X=0, Z) = 0, Q_{s_k}(t, X=1, Z) = K_s C_{s_k}(t, Z) \text{ (equilibrium conditions)}, Z \in \Omega_k, k = \overline{1, N+1}. \tag{14}$$

Additional condition (NMR-*experimental data*)

$$\left[C_{s_k}(t, Z) + \overline{Q}_{s_k}(t, Z)\right]\big|_{h_k} = M_{s_k}(t, Z)\big|_{h_k}, \; s = \overline{1, 2}; h_k \in \Omega_k. \tag{15}$$

The problem of the calculation (9)–(15) is to find unknown functions $D_{\text{intra}_s} \in \Omega_t, D_{\text{inter}_s} \in \Omega_t$ ($D_{\text{intra}_s} > 0, D_{\text{inter}_s} > 0, s = \overline{1, 2}$), when absorbed masses $C_{s_k}(t, Z) + \overline{Q}_{s_k}(t, Z)$ satisfy the condition (15) for every point $h_k \subset \Omega_k$ of the kth layer [8, 12].

Here

$$\mathrm{e}_{\text{inter}_k} = \frac{\varepsilon_{\text{inter}_k} c_{sk}}{\varepsilon_{\text{inter}_k} c_{sk} + \left(1 - \varepsilon_{\text{inter}_k}\right) q_{sk}} \approx \frac{\varepsilon_{\text{inter}_k}}{\left(1 - \varepsilon_{\text{inter}_k}\right) \tilde{\mathrm{K}}_{sk}}, \tilde{\mathrm{K}}_{s_k} = \frac{\mathrm{q}_{s_k \infty}}{\mathrm{c}_{s_k \infty}},$$

where $\overline{Q}_s(t, Z) = \int_0^1 Q_s(t, X, Z) X dX$ is the average concentration of adsorbed component s in micropores and $M_s(t, Z)|_{h_k}$ is the experimental distribution of the mass of the sth component absorbed in macro- and micropores at $h_k \subset \Omega_k$ (results of NMR data, **Figure 2**).

4.3 Iterative gradient method of co-diffusion coefficient identification

The calculation of $D_{\text{intra}_{s_k}}$ and $D_{\text{inter}_{s_k}}$ is a complex mathematical problem. In general, it is not possible to obtain a correct formulation of the problem (9)–(15) and to construct a unique analytical solution, because of the complexity of taking into account all the physical parameters (variation of temperature and pressure, crystallite structures, nonlinearity of Langmuir isotherms, etc.), as well as the insufficient number of reliable experimental data, measurement errors, and other factors.

Therefore, according to the principle of Tikhonov and Arsenin [13], later developed by Lions [14] and Sergienko et al. [15], the calculation of diffusion coefficients requires the use of the model for each iteration, by minimizing the difference between the calculated values and the experimental data.

The calculation of the diffusion coefficients (9)–(15) is reduced to the problem of minimizing the functional of error (16) between the model solution and the experimental data, the solution being refined incrementally by means of a special calculation procedure which uses fast high-performance gradient methods [6, 8, 12, 15].

According to [12, 15], and using the error minimization gradient method for the calculation of $D_{\text{intra}_{s_k}}$ and $D_{\text{inter}_{s_k}}$ of the sth diffusing component, we obtain the iteration expression for the n + 1th calculation step:

$$D^{n+1}_{\text{intra}_{s_k}}(t) = D^{n}_{\text{intra}_{s_k}}(t) - \nabla J^{n}_{D_{\text{intra}_{s_k}}}(t)$$

$$\frac{\left[C_{s_k}\left(D^n_{\text{inter}_{s_k}}, D^n_{\text{intra}_{s_k}}; t, h_k\right) + \overline{Q}_{s_k}\left(D^n_{\text{inter}_{s_k}}, D^n_{\text{intra}_{s_k}}; t, h_k\right) - M_{s_k}(t)\right]^2}{\left\|\nabla J^n_{D_{\text{intra}_{s_k}}}(t)\right\|^2 + \left\|\nabla J^n_{D_{\text{inter}_{s_k}}}(t)\right\|^2},$$

$$D^{n+1}_{\text{inter}_{s_k}}(t) = D^{n}_{\text{inter}_{s_m}}(t) - \nabla J^{n}_{D_{\text{inter}_{s_k}}}(t)$$

$$\frac{\left[C_{s_k}\left(D^n_{\text{inter}_{s_k}}, D^n_{\text{intra}_{s_k}}; t, h_k\right) + \overline{Q}_{s_k}\left(D^n_{\text{inter}_{s_k}}, D^n_{\text{intra}_{s_k}}; t, h_k\right) - M_{s_k}(t)\right]^2}{\left\|\nabla J^n_{D_{\text{intra}_{s_k}}}(t)\right\|^2 + \left\|\nabla J^n_{D_{\text{inter}_{sk}}}(t)\right\|^2}, \quad t \in \left(0, t^{total}\right) \tag{16}$$

where $J\left(D_{\text{inter}_{s_k}}, D_{\text{intra}_{s_k}}\right)$ is the error functional, which describes the deviation of the model solution from the experimental data on $h_k \in \Omega_k$, which is written as

$$J\left(D_{\text{inter}_{s_k}}, D_{\text{intra}_{s_k}}\right) = \frac{1}{2}\int_0^T \left[C_s\left(\tau, Z, D_{\text{inter}_{s_k}}, D_{\text{intra}_{s_k}}\right) + \overline{Q}_s\left(t, Z, D_{\text{inter}_{s_k}}, D_{\text{intra}_{s_k}}\right) - M_{s_k}(t)\right]^2_{h_k} d\tau,$$
$$h_k \in \Omega_k, k = \overline{1, N+1}, \tag{17}$$

$\nabla J^n_{D_{\text{intter}_{s_k}}}(t)$, $\nabla J^n_{D_{\text{intra}_{s_k}}}(t)$ (the gradients of the error functional), $J\left(D_{\text{inter}_{s_k}}, D_{\text{intra}_{s_k}}\right)$.

$\left\|\nabla J^n_{D_{\text{inter}_{sk}}}(t)\right\|^2 = \int_0^T \left[\nabla J^n_{D_{\text{inter}_{sk}}}(t)\right]^2 dt$, $\left\|\nabla J^n_{D_{\text{intra}_{sk}}}(t)\right\|^2 = \int_0^T \left[\nabla J^n_{D_{\text{intra}_{sk}}}(t)\right]^2 dt$.

4.4 Analytical method of co-diffusion coefficient identification

With the help of iterative gradient methods on the basis of the minimization of the residual functional, very precise and fast analytical methods have been developed making it possible to express the diffusion coefficients in the form of time-dependent analytic functions (16). For their efficient use, it is necessary to have an extensive experimental database, with at least two experimental observation conditions for the simultaneous calculation of $D_{\text{intra}_{s_k}}$ and $D_{\text{inter}_{s_k}}$ coefficients. Our experimental studies were carried out for five Z positions of the swept zeolite layer for each of the adsorbed components. The data were not sufficient to fully apply this simultaneous identification method to these five sections. We therefore used a combination of the analytical method and the iterative gradient method for determining the co-diffusion coefficients.

Using Eqs. (9)–(15), it is possible to calculate $D_{\text{intra}_{s_k}}, D_{\text{inter}_{sk}}$ as a function of time using the experimental data obtained by NMR scanning. In particular, in Eqs. (9) and (10), the co-diffusion coefficients can be set directly as functions of the time t: $D_{\text{intra}_{s_k}}(t), D_{\text{inter}_{sk}}(t)$. In this case, the boundary condition (11) can be given in a more general form—also as a function of time:

$$C_{s_1}(t, 1) = C_s^{initial}(t). \tag{18}$$

Experimental NMR scanning conditions are defined simultaneously for all P observation surfaces:

$$\left[C_{sk}(t, Z) + \int_0^1 Q_{sk}(t, X, Z)dX\right]_{Z=h_i} = M_{sk_i}(t, Z)\big|_{h_i}, i = \overline{1, P}, s = \overline{1, 2}; h_i \in \bigcup_{k=1}^{N+1} \Omega_k \tag{19}$$

For simplicity we design $u(t, Z) = C_{sk}(t, Z), v(t, \mathrm{X}, Z) = Q_{sk}(t, \mathrm{X}, Z)$,

$$b(t) = D_{\text{intra}_{sk}}(t)/\mathrm{R}^2, \chi_i(t) = M_{sk_i}(t), i = \overline{1,\mathrm{P}},$$

and considering Eq. (10) in flat form, its solution can be written as [16]:

$$v(t,\mathrm{X},\mathrm{Z}) = -\int_0^t \mathcal{H}_{4\xi}^{(2)}(t,\tau,\mathrm{X},1))b(\tau)u(\tau,\mathrm{Z})d\tau \tag{20}$$

where $\mathcal{H}_{4\xi}^{(2)}(t,\tau,\mathrm{X},\xi) = -2\sum_{m=0}^{\infty} e^{-\eta_m^2(\theta_2(\mathrm{t})-\theta_2(\tau))}\eta_m \cos\eta_m X \cdot (-1)^m$.

Here the Green influence function of the particle $\mathcal{H}_k^{(2)}, \overline{k=1,4}$ is used; it has the form [17].

$$\mathcal{H}_4^{(2)}(t,\tau,\mathrm{X},\xi) = 2\sum_{m=0}^{\infty} e^{-\eta_m^2(\theta_2(\mathrm{t})-\theta_2(\tau))}\cos\eta_m X\cos\eta_m\xi, \eta_m = \tfrac{2m+1}{2}\pi,$$

$$\mathcal{H}_3^{(2)}(t,\tau,\mathrm{X},\xi) = 2\sum_{m=0}^{\infty} e^{-\eta_m^2(\theta_2(\mathrm{t})-\theta_2(\tau))}\sin\eta_m X\sin\eta_m\xi, \eta_m = \frac{2m+1}{2}\pi,$$

$$\mathcal{H}_2^{(2)}(t,\tau,\mathrm{X},\xi) = 1 + 2\sum_{m=1}^{\infty} e^{-\eta_m^2(\theta_2(\mathrm{t})-\theta_2(\tau))}\cos\eta_m X\cdot\ \cos\eta_m\xi, \eta_m = m\pi,$$

where $\theta_2(t) = \int_0^t b(s)ds$.

The notation $\mathcal{H}_{4\tau\xi}^{(2)}, \mathcal{H}_{4\xi\xi}^{(2)}$ means partial derivatives of the influence function $\mathcal{H}_4^{(2)}$ relative to the definite variables τ and ξ, respectively.

Based on formula (20), we calculate

$$v_X(t,\mathrm{X},\mathrm{Z}) = -\int_0^t \mathcal{H}_{4\xi X}^{(2)}(t,\tau,\mathrm{X},1)b(\tau)u(\tau,\mathrm{Z})d\tau \tag{21}$$

Integrating parts (21), taking into account the relations.

$$\mathcal{H}_{4X}^{(2)}(t,\tau,\mathrm{X},\xi) = -\mathcal{H}_{3\xi}^{(2)}(t,\tau,X,\xi), \mathcal{H}_{3\tau}^{(2)}(t,\tau,X,\xi) = -b(\tau)\mathcal{H}_{3\xi\xi}^{(2)}(t,\tau,X,\xi),$$

and the initial condition $u_{|t=0} = 0$, we find

$$v_X(t,\mathrm{X},\mathrm{Z}) = \int_0^t \mathcal{H}_3^{(2)}(t,\tau,\mathrm{X},1))u_\tau(\tau,\mathrm{Z})d\tau \tag{22}$$

We substitute the expression $v(t,\mathrm{X},\mathrm{Z})$ (20) in the observation conditions (19):

$$u(t,h_i) - \int_0^1 XdX\int_0^t \mathcal{H}_{4\xi}^{(2)}(t,\tau,\mathrm{X},1)b(\tau)u(\tau,h_i)d\tau = \chi_i(\mathrm{t}), i = \overline{1,\mathrm{P}} \tag{23}$$

Integrating parts (23) and taking into account equality

$$\mathcal{H}_{4\xi}^{(2)}(t,\tau,X,1) = -\mathcal{H}_{3X}^{(2)}(t,\tau,X,1),$$

we obtain [16]

$$u(t,h_i) = \chi_i(\mathrm{t}) - \int_0^t \mathcal{H}_3^{(2)}(t,\tau,1,1)b(\tau)u(\tau,h_i)d\tau + \int_0^t\int_0^1 \mathcal{H}_3^{(2)}(t,\tau,\mathrm{X},1)b(\tau)u(\tau,h_i)dXd\tau, i = \overline{1,\mathrm{P}} \tag{24}$$

Let us first put $u(t,h_P) = \mu_{sP}(t) = C_s^{initial}(t)$, where $Z = h_P$ is the observation surface, approaching the point of entry into the work area Z = 1.

Then Eq. (24) for $i = P$ will be

$$\int_0^t \mathcal{H}_3^{(2)}(t,\tau,1,1)b(\tau)\mu_{sP}(t)d\tau = \chi_{sP}(t) - \mu_{sP}(t) + \int_0^t\int_0^1 \mathcal{H}_3^{(2)}(t,\tau,\mathrm{x},1)b(\tau)\mu_{sP}(t)dxd\tau \tag{25}$$

Applying to Eq. (25) the formula $\int_\tau^t b(\sigma)\mathcal{H}_2^{(2)}(t,\sigma,0,0))\mathcal{H}_4^{(2)}(t,\sigma,0,0))d\sigma = 1$, obtained by Ivanchov [16], and taking into account.

$\mathcal{H}_3^{(2)}(t,\sigma;1,1) = \mathcal{H}_4^{(2)}(t,\sigma;0,0)$, we obtain

$$\int_0^t b(\tau)\mu_{sP}(\tau)d\tau = \int_0^t \mathcal{H}_2^{(2)}(t,\sigma,0,0)b(\sigma)(\chi_{sP}(\sigma) - \mu_{sP}(\sigma))d\sigma + \int_0^t \mathcal{H}_2^{(2)}(t,\sigma,0,0)b(\sigma)d\sigma\int_0^\sigma\int_0^1 \mathcal{H}_3^{(2)}(\sigma,\tau,\mathrm{x},1)b(\tau)\mu_{sP}(t)dXd\tau, t\in\left[0,t^{total}\right] \tag{26}$$

Differentiating Eq. (26) by t, after the transformations series, we obtain

$$\mu_{sP}(t) = \int_0^t \mathcal{H}_2^{(2)}(t,\sigma,0,0)(b(\sigma)\mu_{sP}(\sigma) + \chi_{sP}(\sigma) - \mu_{sP}(\sigma))d\sigma \tag{27}$$

After multiplying Eq. (27) on the expression $\mathcal{H}_4^{(2)}(t,\sigma,0,0))b(\sigma)$, the integration by τ and the differentiation by t

$$b(t)\mu_{sP}(t) + \chi_{sP}(\sigma) - \mu_{sP}(\sigma) = b(t)\int_0^t \mathcal{H}_2^{(2)}(t,\tau,0,0))\mu'_{sP}(\tau))d\tau.$$

So we obtain the expression for calculating the co-diffusion coefficient in the intra-crystallite space:

$$D_{\mathrm{intra}_{sP}}(t) \equiv R^2 b(t) = R^2\frac{\chi'_{sP}(t) - \mu'_{sP}(t)}{\int_0^t \mathcal{H}_2^{(2)}(t,\tau,0,0))\mu'_{sP}(\tau)d\tau - \mu_{sP}(t)}, t\in\left[0,t^{total}\right] \tag{28}$$

Using calculated $D_{\mathrm{intra}_{sP}}(t)$ with the formula (28) on the observation limit h_P, we define the gradient method $D_{\mathrm{inter}_{sP}}(t)$ in the same way. With $D_{\mathrm{intra}_{sP}}(t)$ and $D_{\mathrm{inter}_{sP}}(t)$ in h_P, we calculate $C_{sk}(t,h_P)$, substituting it in $\mu_{sP-1}(t) = C_{sk}(t,h_P)$ for the next

coefficient $D_{\text{inter}_{si}}(t), i = \overline{P-1,1}$ calculations. All subsequent coefficients $D_{\text{intra}_{si}}(t)$ will be calculated by the formula

$$D_{\text{intra}_{si}}(t) \equiv R^2 b_{si}(t) = R^2 \frac{\chi'_{si}(t) - \mu'_{si}(t)}{\int_0^t \mathcal{H}_2^{(2)}(t,\tau,0,0))\mu'_{si}(\tau)d\tau - \mu_{si}(t)}, i = \overline{P-1,1} \qquad (29)$$

with parallel computing $D_{\text{inter}_{si}}(t), i = \overline{P-1,1}$.

5. Numerical simulation and analysis: co-diffusion coefficients: concentration profiles in inter- and intra-crystallite spaces

The variation against time of the benzene and hexane intra-crystallite diffusion coefficients, $D_{\text{intra}_{1,k}}$ and $D_{\text{intra}_{2,k}}$, respectively, is presented in **Figure 3** for the five coordinate positions: 6, 8, 10, 12, and 14 mm, defined now from the top of the bed. The curves for benzene $D_{\text{intra}_{1,k}}$ are pseudo exponentials. $D_{\text{intra}_{1,k}}$ decreases from 9.0

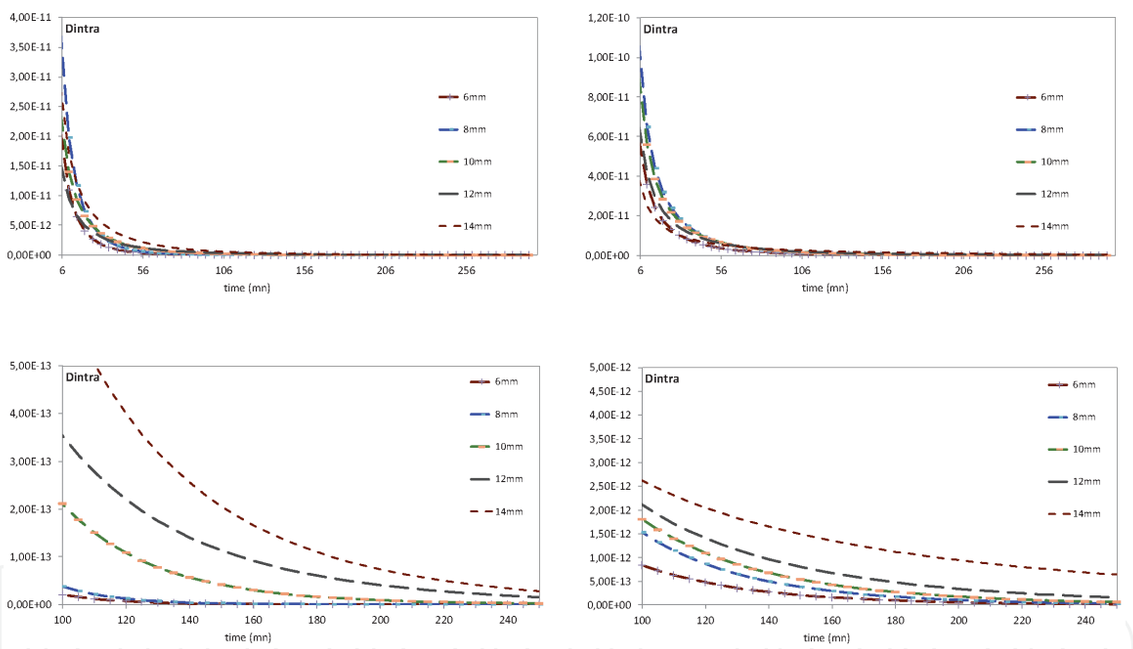

Figure 3.
Variation of intra-crystallite diffusion coefficients (arbitrary units) for benzene $D_{intra_{1,k}}$ (left) and hexane $D_{intra_{2,k}}$ (right) against time, at different positions in the bed. (Top) time range 6–240 mn, (bottom) time range 100–240 mn.

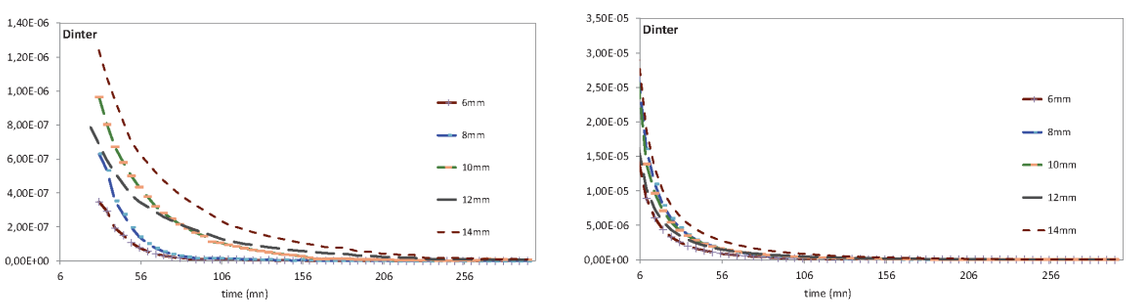

Figure 4.
Variation of inter-crystallite diffusion coefficients (a.u.) for benzene (left) and hexane (right) against time at different positions in the bed.

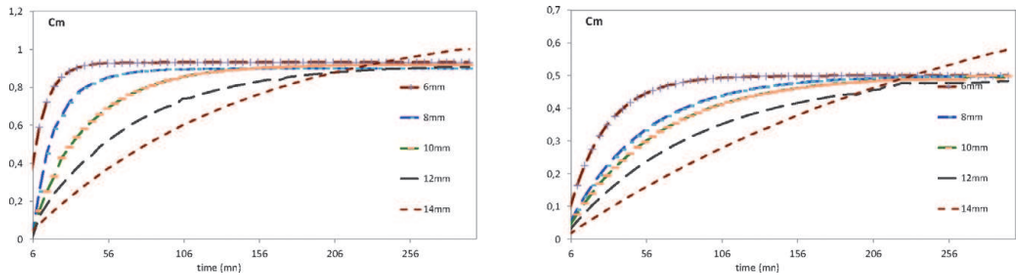

Figure 5.
Variation of the inter-crystallite concentration (a.u.) calculated for benzene (left) and hexane (right) against time and at different positions in the bed.

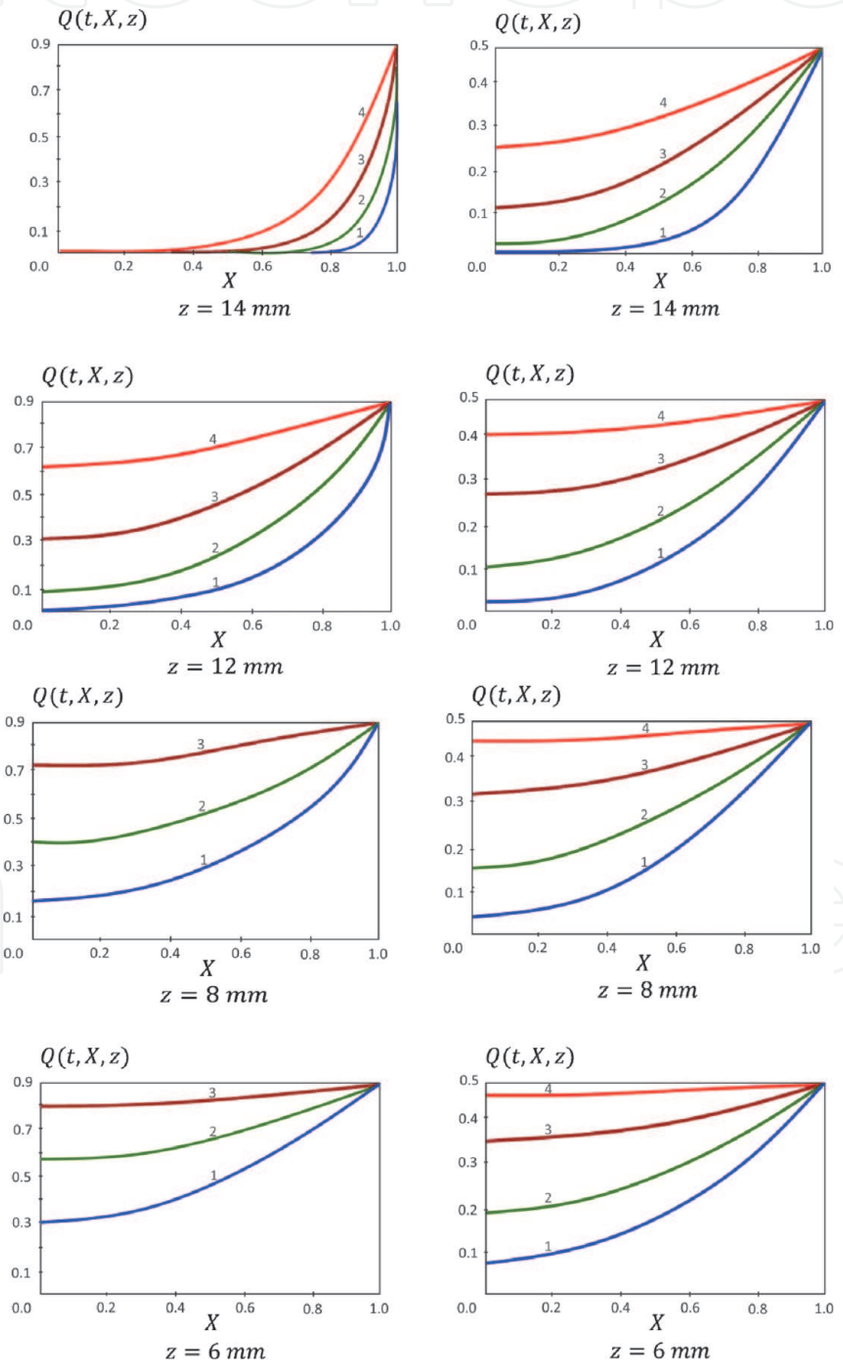

Figure 6.
Distribution of the benzene (left) and hexane (right) concentrations in the intra-crystallite space from the surface (abscissa 1) to the center (abscissa 0) of the crystallites, at different times: (1) dark blue, t = 25 min; (2) green, t = 50 min; (3) brown, t = 100 min; and (4) red, t = 200 min.

E−13 to about 1.0 E−14 a.u. (equilibrium) depending on the position of the crystallite and the time, as well as on the amount of adsorbed gas. The shapes of the variations of $D_{\text{intra}_{2,k}}$ for hexane are roughly the same, but the diffusion coefficients are higher, from about 9.0 E−12 to 3.0 E−13 a.u.

Figure 4 presents the variation against time of the benzene and hexane diffusion coefficients in inter-crystallite space, $D_{\text{inter}_{1,k}}$ and $D_{\text{inter}_{2,k}}$, for the same positions. These coefficients decrease with time from 2.0 E−6 to 1.0 E−7 a.u. (equilibrium) for benzene and from 3 E−5 to 1.0 E−6 a.u. for hexane, depending on the bed position, and increase adsorbed concentrations.

Figure 5 shows the variation against time of the calculated concentrations C for benzene and hexane in the inter-crystallite space. As can be seen, these concentrations approach the equilibrium values for a diffusion time around 250 min. But the variations of the concentrations with time are rather different for the two gases.

Figure 6 shows the variation of the concentrations $Q(t,X,z)$ of adsorbed benzene (left) and hexane (right) in the micropores of the intra-crystallite space from the surface (abscissa-1) to the center (abscissa-0) of the crystallites located between 6 and 14 mm from the top of the bed and after 25–200 min. of diffusion (a, b, c, and d, respectively). The gradients increase, and the mean concentrations decrease with the increasing distance of the particles from the arrival of the gases. The particles at 6 and 8 mm are saturated with benzene after 100 min, but not yet with hexane.

6. Conclusion

The main result of this work is the possibility, from a single experiment, of simultaneously distributing several co-diffusing gases in a porous solid and of using the methods of mathematical modeling to analyze for each of them the distribution of their concentrations in the intra- and inter-crystallite spaces.

Using the experimental NMR data and proposed co-adsorption models, the identification procedures for calculating the co-diffusion coefficients for two or more components in intra- and inter-crystallite spaces are developed. These procedures use the iterative gradual identification methods on minimizing of the Lagrange error function and rapid analytic methods based on the influence function. The co-diffusion coefficients were obtained as a function of time for different positions along the catalyst bed. In particular, those in the intra-crystallite space were computed by the analytical method which allowed a calculation with a relatively high degree of discretization over time and to reduce practically twice the volume of iterative calculations. Using these results, the concentrations of co-diffusing benzene and hexane in the inter- and intra-crystallite spaces were calculated for each time and each position in the bed.

Nomenclature

$k = \overline{1, N+1}$	layer number, subscript k will be added to all the following symbols to specify that they are characteristic of the kth layer
c	adsorbate concentration in macropores
c_∞	equilibrium adsorbate concentration in macropores
$C = c/c_\infty$	dimensionless adsorbate concentration in macropores

D_{inter}	diffusion coefficient in macropores, m^2/s
D_{intra}	diffusion coefficient in micropores, m^2/s
$\tilde{K}$	adsorption equilibrium constant
l	bed length, m
$\Delta l = l_k - l_{k-1}; k = \overline{1, N+1}$	layer thickness (all layers have the same thickness)
L	dimensionless bed length (L = 1)
q	adsorbate concentration in micropores
q_∞	equilibrium adsorbate concentration in micropores
$Q = q/q_\infty$	dimensionless concentration of adsorbate in micropores
T	temperature of gas phase flow, K, and time total, s
M	mass total
u	velocity of gas phase flow, m/s^2
Λ	coefficient of thermal diffusion along the columns
h_g	gas heat capacity, kJ/(kg K)
μ	molecular mass of adsorbate, kg/mol
H	total heat capacity of the adsorbent and gas, kJ/(kg K)
α_h	heat transfer coefficient
R_{column}	column radius, m
R_g	gas constant, kJ mol/(m^3 K)
ΔH_i	activation energy ($\Delta H_i = \Delta \overline{H}_i/\mu$), kJ/mol
$\Delta \overline{H}_i$	adsorption heat, kJ/kg
k_{0i}	empirical equilibrium coefficient for the i adsorbate, depending on the adsorbent properties and the diffusing adsorbate component (k_{0i} equal to the ratio of the desorption and adsorption rate constants)
x	distance from crystallite center, m
R	mean crystallite radius, m (we assume that the crystallites are spherical)
X = x/R	dimensionless distance from crystallite center
z	distance from the bottom of the bed for mathematical simulation, m
$Z = z/l$	dimensionless distance from the bottom of the bed
t	time
τ, ξ	variables of integration
t^{total}	total duration of co-adsorption, mn
L_k	dimensionless position of the kth layer
h_k	$(L_k - L_{k\text{-}1})/2$
ε_{inter}	inter-crystallite bed porosity
e_{inter}	value utilized in Eq. (9)
n	iteration number of identification
m	number of adsorbed components
P	number of NMR observation surfaces
s	index of adsorbate component
i	index of NMR observation surface
initial	index of initial value (concentrations, temperature)
macro	index of extended Lagrange functional component for inter-crystallite space
micro	index of extended Lagrange functional component for intra-crystallite space

Appendix

A. Iterative gradient method of the identification of co-diffusion coefficients

The methodology for solving the direct boundary problem (9)–(15), which describes the diffusion process in a heterogeneous nanoporous bed, is developed in [9, 12, 15]. According to [12] the procedure for determining the diffusion coefficients (16) requires a special technique for calculating the gradients $\nabla J^n_{D_{\text{intra}_{s_k}}}(t)$ and $\nabla J^n_{D_{\text{inter}_{s_k}}}(t)$ of the residual functional (17). This leads to the problem of optimizing the extended Lagrange function [12, 15]:

$$\Phi\left(D_{\text{inter}_{\text{sk}}}, D_{\text{intra}_{\text{sk}}}\right) = J_s + I_{s_{macro}} + I_{s_{micro}}, \tag{A.1}$$

where $I_{s_{macro}}, I_{s_{micro}}$ are the components given by Eqs. (A.2) and (A.3), corresponding to the macro- and microporosity, respectively

$$I_{s_{macro}} = \int_0^T \int_{L_{k-1}}^{L_k} \phi_{s_k}(t,Z)\left(\frac{\partial C_{s_k}}{\partial t} - \frac{D_{\text{inter}_{sk}}}{l^2}\frac{\partial^2 C_{s_k}}{\partial Z^2} + e_{\text{inter}_k} K_{s_k}\frac{D_{\text{intra}_{s_k}}}{R^2}\left(\frac{\partial Q(t,X,Z)_{s_k}}{\partial X}\right)_{X=1}\right) dZdt \tag{A.2}$$

$$I_{s_{micro}} = \int_0^T \int_0^1 \int_{L_{k-1}}^{L_k} \psi_{s_k}(t,X,Z)\left(\frac{\partial Q_{s_k}(t,X,Z)}{\partial t} - \frac{D_{\text{intra}_{sk}}}{R^2}\left(\frac{\partial^2 Q_{s_k}}{\partial X^2} + \frac{2}{X}\frac{\partial Q_{s_k}}{\partial X}\right)\right) XdXdZdt \tag{A.3}$$

J_s is the residual functional (17), $\phi_{s_k}, \psi_{s_k}, {}_{s,=\overline{1,2}}$—unknown factors of Lagrange, to be determined from the stationary condition of the functional $\Phi\left(D_{\text{inter}_{\text{sk}}}, D_{\text{intra}_{\text{sk}}}\right)$ [9, 15]:

$$\Delta\Phi\left(D_{\text{inter}_{\text{sk}}}, D_{\text{intra}_{\text{sk}}}\right) \equiv \Delta J_s + \Delta I_{s_{macro}} + \Delta I_{s_{micro}} = 0 \tag{A.4}$$

The calculation of the components in Eq. (A.4) is carried out by assuming that the values $D_{\text{inter}_{\text{sk}}}, D_{\text{intra}_{\text{sk}}}$ are incremented by $\Delta D_{\text{inter}_{\text{sk}}}, \Delta D_{\text{intra}_{\text{sk}}}$. As a result, concentration $C_{s_k}(t,Z)$ changes by increment $\Delta C_{sk}(t,Z)$ and concentration $Q_{s_k}(t,X,Z)$ by increment $\Delta Q_{s_k}(t,X,Z), s = \overline{1,2}$.

Conjugate problem. The calculation of the increments ΔJ_s, $\Delta J_{s_{macro}}$, and $\Delta J_{s_{micro}}$ in Eq. (A.4) (using integration by parts and the initial and boundary conditions of the direct problem (9)–(15)) leads to solving the additional conjugate problem to determine the Lagrange factors ϕ_{s_k} and ψ_{s_k} of the functional (A.1) [15]:

$$\frac{\partial \phi_{s_k}(t,Z)}{\partial t} + \frac{D_{\text{inter}_{sk}}}{l^2}\frac{\partial^2 \phi_{s_k}}{\partial Z^2} + e_{\text{inter}_k} K_{s_k}\frac{D_{\text{intra}_{s_k}}}{R^2}\frac{\partial \psi_{s_k}(t,X,Z)}{\partial X}\bigg|_{X=1} = E^n_{s_k}(t)\delta(Z-h_k) \tag{A.5}$$

where $E^n_{s_k}(t) = C_{s_k}\left(D_{\text{intra}_{sk\,n}}, D_{\text{inter}_{sk\,n}}; t, h_k\right) + \overline{Q}_{s_k}\left(D_{\text{intra}_{sk\,n}}, D_{\text{inter}_{sk\,n}}; t, h_k\right) - M_{sk}(t)$, $\delta(Z-h_k)$ (function of Dirac) [15].

$$\frac{\partial \psi_{s_k}(t,X,Z)}{\partial t} + \frac{D_{\text{intra}_{sk}}}{R^2}\left(\frac{\partial^2 \psi_{s_k}}{\partial X^2} + \frac{2}{X}\frac{\partial \psi_{s_k}}{\partial X}\right) = E^n_{s_k}(t)\delta(Z-h_k) \tag{A.6}$$

$$\phi_{s_k}(t,Z)_{|t=t^{total}} = 0; \psi_{s_k}(t,X,Z)_{|t=t^{total}} = 0 \ \left(\text{conditions at } t = t^{total}\right); \tag{A.7}$$

$$\frac{\partial}{\partial X}\psi_{s_k}(t,X,Z)_{|X=0} = 0; \psi_{s_k}(t,X,Z)_{|X=1} = \varphi_{s_k}(t,Z) \tag{A.8}$$

$$\phi_{s_k}(t,Z=L_k) = 0, \phi_{s_{k-1}}(t,Z=L_{k-1}) = 0; s = \overline{1,2}, k = \overline{N,2}, \tag{A.9}$$

$$\phi_{s_1}(t,L_1) = 0, \frac{\partial \phi_{s_1}}{\partial Z}(t,Z=0) = 0 \tag{A.10}$$

We have obtained the solutions ϕ_{sk} and ψ_{sk} of problem (A.5)–(A.10) using Heaviside operational method in [15].

Substituting in the direct problem (9)–(15) $D_{\text{inter}_{\text{sk}}}, D_{\text{intra}_{\text{sk}}}$, $C_{s_k}(t,Z)$, and $Q_{s_k}(t,X,Z)$ by the corresponding values with increments $D_{\text{inter}_{\text{sk}}} + \Delta D_{\text{inter}_{\text{sk}}}, D_{\text{intra}_{\text{sk}}} + \Delta D_{\text{intra}_{\text{sk}}}$, $C_{s_k}(t,Z) + \Delta C_{s_k}(t,z)$, and $Q_{s_k}(t,X,Z) + \Delta Q_{s_k}(t,X,Z)$, subtracting the first equations from the transformed ones and neglecting second-order terms of smallness, we obtain the basic equations of the problem (9)–(15) in terms of increments $\Delta C_{s_k}(t,Z)$ and $\Delta Q_{s_k}(t,X,Z), s = \overline{1,2}$ in the operator form

$$\mathcal{L}w_{s_k}(t,X,Z) = \mathrm{X}_{s_k}, w_{s_k} \in (0,1) \cup \Omega_{kt}, k = \overline{1,N+1} \tag{A.11}$$

Similarly, we write the system of the basic equations of conjugate boundary problem (A.5)–(A.10) in the operator:

$$\mathcal{L}^* \Psi_{s_k}(t,X,Z) = E_{s_k}(t)\delta(Z-h_k), \Psi_{s_k} \in (0,1) \cup \Omega_{kt}, k = \overline{1,N+1} \tag{A.12}$$

$$\text{where } \mathcal{L} = \begin{bmatrix} \frac{\partial}{\partial t} - \frac{\partial}{\partial Z}\left(D_{\text{inter}_{\text{sk}}}\frac{\partial}{\partial Z}\right) & e_{\text{inter}_k}\frac{D_{\text{intra}_{\text{sk}}}}{R}\frac{\partial}{\partial X}|_{X=1} \\ 0 & \frac{\partial}{\partial t} - \frac{D_{\text{intra}_{\text{sk}}}}{R^2}\left(\frac{\partial^2}{\partial X^2} + \frac{2}{X}\frac{\partial}{\partial X}\right) \end{bmatrix},$$

$$\mathcal{L}^* = \begin{bmatrix} \frac{\partial}{\partial t} + \frac{\partial}{\partial Z}\left(D_{\text{inter}_{\text{sk}}}\frac{\partial}{\partial Z}\right) & e_{\text{inter}_k}\frac{D_{\text{intra}_{\text{sk}}}}{R^2}\frac{\partial}{\partial X}|_{X=1} \\ 0 & \frac{\partial}{\partial t} + \frac{D_{\text{intra}_{\text{sk}}}}{R^2}\left(\frac{\partial^2}{\partial X^2} + \frac{2}{X}\frac{\partial}{\partial X}\right) \end{bmatrix},$$

$$w_{s_k}(t,X,Z) = \begin{bmatrix} \Delta C_{s_k}(t,Z) \\ \Delta Q_{s_k}(t,X,Z) \end{bmatrix}, \Psi_{s_k}(t,X,Z) = \begin{bmatrix} \phi_{s_k}(t,Z) \\ \psi_{s_k}(t,X,Z) \end{bmatrix}.$$

$$\mathrm{X}_{s_k}(t,X,Z) = \begin{bmatrix} \frac{\partial}{\partial Z}\left(\Delta D_{\text{inter}_{\text{sk}}}\frac{\partial}{\partial Z}C_{s_k}\right) - e_{\text{inter}_k}\frac{\Delta D_{\text{intra}_{\text{sk}}}}{R^2}\frac{\partial}{\partial X}Q_{s_k}(t,X,Z)_{X=1} \\ \frac{\Delta D_{\text{intra}_{\text{sk}}}}{R^2}\left(\frac{\partial^2}{\partial X^2} + \frac{2}{X}\frac{\partial}{\partial X}\right)Q_{s_k}(t,X,Z) \end{bmatrix} \tag{A.13}$$

where $\mathcal{L}^*$ is the conjugate Lagrange operator of operator $\mathcal{L}$.

The calculated increment of the residual functional (17), neglecting second-order terms, has the form

$$\begin{aligned} \Delta J_s\left(D_{\text{intra}_{\text{sk}}}, D_{\text{inter}_{\text{sk}}}\right) = &\int_0^T \int_{L_{k-1}}^{L_k} \mathcal{L}^{-1}\mathrm{X}_{s_{k,1}}(t,Z)\cdot E_{s_k}(t)\delta(Z-h_k)dZdt \\ &+ \int_0^T \int_{L_{k-1}}^{L_k} \int_0^1 \mathcal{L}^{-1}\mathrm{X}_{s_{k2}}(t,X,Z)\cdot E_{s_k}(t)\delta(Z-h_k)XdXdZdt \end{aligned} \tag{A.14}$$

where $w_{s_k} = \mathcal{L}^{-1}\mathrm{X}_{s_k}$ and $\mathcal{L}^{-1}$ is the inverse operator of operator $\mathcal{L}$.
Defining the scalar product

$$\left(\mathcal{L}w_{s_k}(t,X,Z),\Psi_{s_k}(t,X,Z)\right) = \begin{bmatrix} \int\int\limits_{\Omega_{kT}} \mathcal{L}\Delta C_{s_k}(t,Z)\phi_{s_k}(t,Z)dZdt \\ \iiint\limits_{(0,R)\cup\Omega_{kT}} \mathcal{L}\Delta Q_{s_k}(t,X,Z)\psi_{s_k}(t,X,Z)XdXdZdt \end{bmatrix} \tag{A.15}$$

and taking into account (A.19) Lagrange's identity [12, 15]

$$\left(\mathcal{L}w_{s_k}(t,X,Z),\Psi_{s_k}(t,X,Z)\right) = \left(w_{s_k}(t,X,Z),\mathcal{L}^{*}\Psi_{s_k}(t,X,Z)\right) \tag{A.16}$$

and the equality $\mathcal{L}^{-1*}\left[E_{s_k}(t)\delta(Z-h_k)\right] = \Psi_{s_k}$, we obtain the increment of the residual functional expressed by the solution of conjugate problem (A.6)–(A.10) and the vector of the right-hand parts of Eq. (A.13):

$$\Delta J_s\left(D_{\mathrm{inter_{sk}}}, D_{\mathrm{intra_{sk}}}\right) = \left(\Psi_{s_k}(t,X,Z),\mathrm{X}_{s_k}(t,X,Z)\right) \tag{A.17}$$

where $\phi_{s_k}(t,Z)$ and $\psi_{s_k}(t,X,Z)$ belong to $\overline{\Omega}_{kt}$ and $[0,1]\cup\overline{\Omega}_{kt}$, respectively, $\mathcal{L}^{-1*}$ is the conjugate operator to inverse operator $\mathcal{L}^{-1}$, and Ψ_{s_k} is the solution of conjugate problem (A.5)–(A.10).

Reporting in Eq. (A.17) the components $\mathrm{X}_{s_k}(t,X,Z)$ taking into account Eq. (A.18), we obtain the formula which establishes the relationship between the direct problem (9)–(15) and the conjugate problem (A.6)–(A.10) which makes it possible to obtain the analytical expressions of components of the residual functional gradient:

$$\begin{aligned}\Delta J_s\left(D_{\mathrm{intra_{sk}}}, D_{\mathrm{inter_{sk}}}\right) = &\left(\phi_{s_k}(t,Z), \frac{\partial}{\partial Z}\left(\Delta D_{\mathrm{inter_{sk}}}\frac{\partial}{\partial Z}C_{s_k}\right) - e_{\mathrm{inter}_k}\frac{\Delta D_{\mathrm{intra_{sk}}}}{R^2}\frac{\partial}{\partial X}Q_{s_k}(t,X,Z)_{X=1}\right) \\ &+\left(\psi_{s_k}(t,X,Z), \frac{\Delta D_{\mathrm{intra_{sk}}}}{R^2}\left(\frac{\partial^2}{\partial X^2}+\frac{2}{X}\frac{\partial}{\partial X}\right)Q_{s_k}(t,X,Z)\right)\end{aligned} \tag{A.18}$$

Differentiating expression (A.18), by $\Delta D_{\mathrm{intra_{sk}}}$ and $\Delta D_{\mathrm{inter_{sk}}}$, respectively, and calculating the scalar products according to Eq. (A.15), we obtain the required analytical expressions for the gradient of the residual functional in the intra- and inter-crystallite spaces, respectively:

$$\begin{aligned}\nabla J_{D_{\mathrm{intra_{sk}}}}(t) = &-\frac{e_{\mathrm{inter}_k}}{R^2}\int\limits_{L_{k-1}}^{L_k}\frac{\partial}{\partial X}Q_{s_k}(t,1,Z)\phi_{s_k}(t,Z)dZ \\ &+\frac{1}{R^2}\int\limits_{L_{k-1}}^{L_k}\int\limits_{0}^{1}\left(\frac{\partial^2}{\partial X^2}+\frac{2}{X}\frac{\partial}{\partial X}\right)Q_{s_k}(t,X,Z)\psi_{s_k}(t,X,Z)XdXdZ\end{aligned} \tag{A.19}$$

$$\nabla J_{D_{\mathrm{inter_{sk}}}}(t) = \int\limits_{L_{k-1}}^{L_k}\frac{\partial^2 C_{s_k}(t,Z)}{\partial Z^2}\phi_{s_k}(t,Z)dZ \tag{A.20}$$

The formulas of gradients $\nabla J^n_{D_{\mathrm{intra}_{s_k}}}(t)$ and $\nabla J^n_{D_{\mathrm{inter}_{s_k}}}(t)$ include analytical expressions of the solutions of the direct problem (9)–(14) and inverse problem (A.5)–

(A.10). They provide high performance of computing process, avoiding a large number of inner loop iterations by using exact analytical methods [2, 15].

B. The linearization schema of the nonlinear co-adsorption model: system of linearized problems and construction of solutions

The linearization schema of nonlinear co-adsorption (1)–(8) is shown in order to demonstrate the simplicity of implementation for the case of two diffusing components ($m = 2$) and isothermal adsorption. The simplified model (1)–(8) for the case of $m = 2$ is converted into the form

$$\frac{\partial C_s(t,Z)}{\partial t} = \frac{D_{\text{inter}_s}}{l^2}\frac{\partial^2 C_s}{\partial Z^2} - e_{\text{inter}}\tilde{K}_s\frac{D_{\text{intra}_s}}{R^2}\left(\frac{\partial Q_s}{\partial X}\right)_{X=1} \tag{A.21}$$

$$\frac{\partial Q_s(t,X,Z)}{\partial t} = \frac{D_{\text{intra}_s}}{R^2}\left(\frac{\partial^2 Q_s}{\partial X^2} + \frac{2}{X}\frac{\partial Q_s}{\partial X}\right), s = \overline{1,2} \tag{A.22}$$

with initial conditions

$$C_s(t=0,Z) = 0; Q_s(t=0,X,Z) = 0; X \in (0,1), s = \overline{1,2} \tag{A.23}$$

boundary conditions for coordinate X of the crystallite

$$\frac{\partial}{\partial X}Q_s(t,X=0,Z) = 0 \tag{A.24}$$

$$\begin{aligned} Q_1(t,X=1,Z) &= \frac{K_1C_2(t,Z)}{1+K_1C_1(t,Z)+K_2C_2(t,Z)} \quad \text{(Langmuir equilibrium)},\\ Q_2(t,X=1,Z) &= \frac{K_2C_2(t,Z)}{1+K_1C_1(t,Z)+K_2C_2(t,Z)} \end{aligned} \tag{A.25}$$

boundary and interface conditions for coordinate Z

$$C_s(t,1) = 1, \frac{\partial C_s}{\partial Z}(t,Z=0) = 0, t \in \left(0,t^{total}\right) \tag{A.26}$$

$K_1 = \frac{\overline{\theta}_1}{p_1\left(1-\overline{\theta}_1-\overline{\theta}_2\right)}, K_2 = \frac{\overline{\theta}_2}{p_2\left(1-\overline{\theta}_1-\overline{\theta}_2\right)}$, where p_1, p_2 are the co-adsorption equilibrium constants and partial pressure of the gas phase for 1-th and 2-th component and $\overline{\theta}_1, \overline{\theta}_2$, are the intra-crystallite spaces occupied by the corresponding adsorbed molecules. The expression $\varphi_s(C_1,C_2) = \frac{C_s(t,Z)}{1+K_1C_1(t,Z)+K_2C_2(t,Z)}$ is represented by the series of Tailor [5]:

$$\begin{aligned} \varphi_s(C_1,C_2) = \varphi_s(0,0) &+ \left(\left.\frac{\partial\varphi_s}{\partial C_1}\right|_{(0,0)}C_1 + \left.\frac{\partial\varphi_s}{\partial C_2}\right|_{(0,0)}C_2\right)\\ &+ \frac{1}{2!}\left(\begin{array}{l}\left.\frac{\partial^2\varphi_s}{\partial C_1^2}\right|_{(0,0)}C_1^2 + 2\left.\frac{\partial^2\varphi_s}{\partial C_1C_2}\right|_{(0,0)}C_1C_1 +\\ \qquad\qquad +\left.\frac{\partial^2\varphi_s}{\partial C_2^2}\right|_{(0,0)}C_2^2\end{array}\right) + \ldots \end{aligned} \tag{A.27}$$

As a result of transformations, limiting to the series not higher than the second order, we obtain

$$\frac{K_1C_1(t,Z)}{1+K_1C_1(t,Z)+K_2C_2(t,Z)} = K_1C_1(t,Z) - \left(K_1^2C_1^2(t,Z) + \frac{1}{2}K_1K_2C_1(t,Z)C_2(t,Z)\right),$$
$$\frac{K_2C_2(t,Z)}{1+K_1C_1(t,Z)+K_2C_2(t,Z)} = K_2C_2(t,Z) - \left(\frac{1}{2}K_1K_2C_1^2(t,Z)C_2^1(t,Z) + K_2^2C_2^2(t,Z)\right) \tag{A.28}$$

Substituting the expanded expression (A.28) in Eq. (A.25) of nonlinear systems (A.20)–(A.26), we obtain

$$Q_1(t,\mathrm{X},Z)_{X=1} = K_1C_1(t,Z) - \varepsilon\left(C_1^2(t,Z) + \frac{1}{2}\frac{K_2}{K_1}C_1(t,Z)C_2(t,Z)\right),$$
$$Q_2(t,\mathrm{X},Z)_{X=1} = K_2C_2(t,Z) - \varepsilon\left(\frac{1}{2}\frac{K_2}{K_1}C_1(t,Z)C_2(t,Z) + \left(\frac{K_2}{K_1}\right)^2C_2^2(t,Z)\right) \tag{A.29}$$

where $\varepsilon = K_1^2 << 1$ is the small parameter.

Taking into account the approximate equations of the kinetics of co-adsorption (A.29) containing the small parameter ε, we search for the solution of the problem (A.21)–(A.26) by using asymptotic series with a parameter ε in the form [6, 7]

$$C_s(t,\mathrm{Z}) = C_{s_0}(t,\mathrm{Z}) + \varepsilon C_{s_1}(t,\mathrm{Z}) + \varepsilon^2 C_{s_2}(t,\mathrm{Z}) + \ldots, \tag{A.30}$$
$$Q_s(t,X,Z) = Q_{s_0}(t,X,Z) + \varepsilon Q_{s_1}(t,X,Z) + \varepsilon^2 Q_{s_2}(t,X,Z) + \ldots, s = \overline{1,2} \tag{A.31}$$

As the result of substituting the asymptotic series (A.30)–(A.31) into the equations of the nonlinear boundary problem (A.21)–(A.26) considering Eq. (A.28), the problem (A.21)–(A.26) will be parallelized into two types of linearized boundary problems [6]:

The problem $A_{s_0}, s = \overline{1,2}$ (*zero approximation with initial and boundary conditions of the initial problem*): to find a solution in the domain $D = \{(t,\mathrm{X},\mathrm{Z}) : t>0, X \in (0,1), Z \in (0,1)\}$of a system of partial differential equations

$$\frac{\partial C_{s_0}(t,Z)}{\partial t} = \frac{D_{\mathrm{inter}_s}}{l^2}\frac{\partial^2 C_{s_0}}{\partial Z^2} - e_{\mathrm{inter}}\tilde{K}_s\frac{D_{\mathrm{intra}_s}}{R^2}\left(\frac{\partial Q_{s_0}}{\partial X}\right)_{X=1} \tag{A.32}$$
$$\frac{\partial Q_{s_0}(t,X,Z)}{\partial t} = \frac{D_{\mathrm{intra}_s}}{R^2}\left(\frac{\partial^2 Q_{s_0}}{\partial X^2} + \frac{2}{X}\frac{\partial Q_{s_0}}{\partial X}\right) \tag{A.33}$$

with initial conditions.

$$C_{s_0}(t=0,Z) = 0; Q_{s_0}(t=0,X,Z) = 0; X \in (0,1), s = \overline{1,2} \tag{A.34}$$

boundary conditions for coordinate X of the crystallite

$$\frac{\partial}{\partial X}Q_{s_0}(t,X=0,Z) = 0 \tag{A.35}$$
$$Q_{s_0}(t,X=1,Z) = K_sC_{s_0}(t,Z), s = \overline{1,2} \tag{A.36}$$

boundary and interface conditions for coordinate Z.

$$C_{s_0}(t,1)=1,\ \frac{\partial C_{s_0}}{\partial Z}(t,Z=0)=0, t\in(0,T) \tag{A.37}$$

The problem $A_n; n=\overline{1,\infty}$ (nth *approximation with zero initial and boundary conditions*): to construct in the domain D a solution of a system of equations

$$\frac{\partial C_{s_n}(t,Z)}{\partial t}=\frac{D_{\text{inter}_s}}{l^2}\frac{\partial^2 C_{s_n}}{\partial Z^2}-e_{\text{inter}}\tilde{K}_s\frac{D_{\text{intra}_s}}{R^2}\left(\frac{\partial Q_{s_n}}{\partial X}\right)_{X=1} \tag{A.38}$$

$$\frac{\partial Q_{s_n}(t,X,Z)}{\partial t}=\frac{D_{\text{intra}_s}}{R^2}\left(\frac{\partial^2 Q_{s_n}}{\partial X^2}+\frac{2}{X}\frac{\partial Q_{s_n}}{\partial X}\right) \tag{A.39}$$

with initial conditions.

$$C_{s_n}(t=0,Z)=0; Q_{s_n}(t=0,X,Z)=0; s=\overline{1,2} \tag{A.40}$$

boundary conditions for coordinate X of the crystallite.

$$\frac{\partial}{\partial X}Q_{s_n}(t,X=0,Z)=0 \tag{A.41}$$

$$Q_{1_n}(t,X,Z)_{X=1}=K_1C_{1_n}(t,Z)-\sum_{\nu=0}^{n-1}C_{1_v}(t,\mathrm{Z})\left(C_{1,n-1-\nu}(t,\mathrm{Z})+\frac{1}{2}\frac{K_2}{K_1}C_{2,n-1-\nu}(t,\mathrm{Z})\right),$$
$$Q_{2_n}(t,X,Z)_{X=1}=K_2C_{2_n}(t,Z)-\sum_{\nu=0}^{n-1}C_{2_s}(t,\mathrm{Z})\left(\frac{1}{2}\frac{K_2}{K_1}C_{1,n-1-\nu}(t,\mathrm{Z})+\left(\frac{K_2}{K_1}\right)^2C_{2,n-1-\nu}(t,\mathrm{Z})\right) \tag{A.42}$$

boundary and interface conditions for coordinate Z.

$$C_{s_n}(t,1)=0,\ \frac{\partial C_{s_0}}{\partial Z}(t,Z=0)=0, t\in\left(0,t^{total}\right) \tag{A.43}$$

The problems $A_{s_0}, s=\overline{1,2}$ are linear with respect to zero approximation C_{s_0}, Q_{s_0}; the problems $A_{s_n}; \mathrm{n}=\overline{1,\infty}$ are linear with respect to the n-th approximation C_{s_n}, Q_{s_n} and nonlinear with respect to all previous *n-1* approximations $C_{s_0}, \ldots, C_{s_{n-1}}$.

As demonstrated for the two-component adsorption model (A.21)–(A.26), our proposed methodology can easily be developed and applied to the co-adsorption of any number of gases.

Author details

Mykhaylo Petryk[1*], Mykola Ivanchov[2], Sebastian Leclerc[3], Daniel Canet[3] and Jacques Fraissard[4]

1 Ternopil Ivan Puluj National Technical University, Ternopil, Ukraine

2 Ivan Franco National University of Lviv, Lviv, Ukraine

3 University of Lorraine, Vandoeuvre-les-Nancy, France

4 Faculty of Science and Engineering, ESPCI, Sorbonne University, Paris, France

*Address all correspondence to: mykhaylo_petryk@tu.edu.te.ua

References

[1] Leclerc S, Trausch G, Cordier B, Grandclaude D, Retournard A, Fraissard J, et al. Chemical shift imaging (CSI) by precise object displacement. Magnetic Resonance in Chemistry. 2006;**44**:311-317

[2] Petryk M, Leclerc S, Canet D, Fraissard J. Mathematical modeling and visualization of gas transport in a zeolite bed using a slice selection procedure. Diffusion Fundamentals. 2007;**4**:11.1. Available from: http://www.diffusion-fundamentals.org

[3] Petryk M, Leclerc S, Canet D, Fraissard J. Modeling of gas transport in a microporous solid using a sclice selection procedure: Application to the diffusion of benzene in ZSM5. Catalysis Today. 2008;**139**:234-240

[4] Leclerc S, Petryk M, Canet D, Fraissard J. Competitive diffusion of gases in a zeolite using proton NMR and a slice selection procedure. Catalysis Today. 2012;**187**:104-107

[5] Petryk MR, Khimich OM, Boyko IV, Mykhalyk DM, Petryk MM, Kovbashyn VI. Mathematical Modeling of Heat Transfer and Adsorption of Hydrocarbons in Nanoporous Media of Exhaust Gas Neutralization Systems. Kyiv: National Academy of Sciences of Ukraine; 2018. p. 280

[6] Petryk M, Khimitch A, Petryk MM. Simulation of adsorption and desorption of hydrocarbons in nanoporous catalysts of neutralization systems of exhaust gases using nonlinear langmuir isotherm. Journal of Automation and Information Sciences, Begell House USA. 2018;**50**(10):18-33

[7] Petryk M, Khimitch A, Petryk MM, Fraissard J. Experimental and computer simulation studies of dehydration on microporous adsorbent of natural gas used as motor fuel. Fuel. 2019;**239**: 1324-1330

[8] Petryk M, Leclerc S, Canet D, Sergienko I, Deineka V, Fraissard J. Competitive diffusion of gases in a zeolite bed: NMR and slice selection procedure, modelling and parameter identification. The Journal of Physical Chemistry C. ACS (USA). 2015;**119**(47): 26519-26525

[9] Deineka V, Petryk M, Fraissard J. Identifying kinetic parameters of mass transfer in components of multicomponent heterogeneous nanoporous media of a competitive diffusion system. Cybernetics and System Analysis Springer. 2011;**47**(5): 705-723

[10] Ruthven DM. Principles of Adsorption and Adsorption Processes. New York: John Wiley; 1984. 433 p

[11] Kärger J, Ruthven D, Theodorou D. Diffusion in Nanoporous Materials. Hoboken: John Wiley & Sons; 2012. 660 p

[12] Sergienko IV, Deineka VS. Optimal Control of Distributed Systems with Conjugation Conditions. New York: Kluwer Academic Publishers; 2005

[13] Tikhonov AN, Arsenin VY. Solutions of Ill-Posed Problems. Washington D.C.: V.H. Winston; New York: J. Wiley; 1977

[14] Lions J-L. Perturbations Singulières Dans les Problèmes Aux Limites et en Contrôle Optimal. New York: Springer; 2008. Lecture Notes in Math. Ser

[15] Sergienko IV, Petryk MR, Leclerc S, Fraissard J. Highly efficient methods of the identification of competitive diffusion parameters in inhomogeneous media of nanoporous particles. Cybernetics and Systems Analysis Springer. 2015;**51**(4):529-546

[16] Ivanchov M. Inverse Problems for Equations of Parabolic Type. Mathematical Studies. Monograph Series. Vol. 10. Lviv: VNTL Publishers; 2003

[17] Lenyuk M, Petryk M. The Methods of Integral Transforms of Fourier-Bessel with Spectral Parameter in Problems of Mathematical Modeling of the Mass Exchange Process in Heterogeneous Medias. Kyiv: Naukova Dumka; 2000